

# Chapter 3

## AC Calorimetry

### 3.1 Experimental methods for the measurement of Specific Heat

In this chapter we compare and contrast the different methods available for the measurement of specific heat. This discussion is basically to choose the best possible method for the measurement of specific heat at high pressures.

The various experimental methods which have been used for the measurement of specific heat are:

- 1) Adiabatic calorimetry
- 2) Pulse methods
- 3) Differential scanning calorimetry
- 4) AC calorimetry

#### 3.1.1 Adiabatic Calorimetry

This is one of the oldest methods for the measurement of specific heat. The basic principle of this method is that a steady heat input is supplied to the sample and the resultant temperature rise of the sample is measured. By equating the heat supplied to the sample and the temperature rise, the specific heat of the sample can be calculated.

$$Q = mC_p\Delta T \quad (3.1)$$

Where Q is the heat supplied to sample

m = Mass of the sample

$C_p$  = Specific heat of the sample

$\Delta T$  = Temperature rise

The basic assumption here is that the entire heat supplied is taken up in raising the temperature of the sample, i.e., there is no heat loss from the sample to the surroundings. If there is any heat loss this has to be taken into account.

The drawback of this method is that complete thermal isolation of the sample from the surroundings is very difficult to achieve especially in a high pressure environment. In a high pressure arrangement, the sample has to be in close contact with the pressure transmitting medium, which is contradictory to the condition stated above. Corrections for the heat loss to the surroundings are difficult to calculate.

### 3.1.2 Pulse methods

In the electric pulse technique, which is generally used for electrical conductors, a wire specimen is heated by a current pulse of the order of 50 Amperes for a duration of about  $100 \mu \text{ Sec}$  [1]. The resulting temperature rise is extracted from the voltage drop across the sample by means of a bridge circuit.

The disadvantage of this method is that the heating and the measuring times have to be kept short. This is done in order to avoid excessive heat losses. In spite of these precautions corrections have to be made for the heat loss to the medium surrounding the wire. Since a pulse of very short duration is used there will be induced voltages in the circuit. These effects have also to be corrected for. This method is not very suitable for studying critical phenomena, since the short measurement time used here conflicts with the large equilibration times necessary near  $T_c$ .

### 3.1.3 Differential Scanning Calorimetry

In this method, the reference material is heated at a constant rate. The sample and the reference are maintained at the same temperature by supplying different quantities of heat to them. A Differential Scanning Calorimeter measures the energy change in the sample directly and the final plot is between differential power (difference in rate of energy supply) and temperature or time.

Determination of the specific heat of the sample is done in two steps. First a DSC curve is taken in the absence of the sample, i.e. with empty pans on both sample and in the reference base. The addition of a sample produces an endothermic displacement relative to the blank baseline which is proportional to the specific heat of the sample.

The displacement,  $d$ , between the baseline in the absence of a sample and the sample trace is given by the equation

$$d = KC_p m dT/dt \quad (3.2)$$

Where  $K$  is a calibration constant,  $C_p$  is the specific heat of the sample,  $m$  is the

sample mass and  $dT/dt$  is the rate of heating. The calibration constant is determined using a standard material of known specific heat, e.g Sapphire.

The disadvantage of this method for studying critical phenomena is that, the sample not in thermodynamic equilibrium for the heating rates normally used in commercial DSC equipments. Near the critical point, the relaxation time of the excitations in the sample becomes very large and the heating rates which are normally used in commercial DSC instruments ( $\sim$  a few  $^{\circ}$  C/min) are no longer suitable for making measurements. Also this method requires a suitable reference material for the determination of the absolute value of the specific heat.

Recently a modification of the DSC technique known as modulated DSC [2] has been used to get information which i

#### 3.1.4 AC Calorimetry

This method rectifies some of the defects of the methods discussed above and has certain features which make it very attractive for the study of critical phenomena. Since this method has been extensively used in the work discussed in subsequent chapters, it will be discussed in greater detail than the other methods.

The basic principle of this method is that a periodic heat input is supplied to the sample. It can be shown that the resultant equilibrium temperature of the sample contains a dc part and an ac part. The amplitude of the temperature oscillations is inversely proportional to the specific heat of the sample.

This method was originally developed by Sullivan and Seidel [3] in 1968. They developed this method to solve some of the problems in low-temperature calorimetry, where the problems of thermal isolation of the sample are more acute than in room temperature calorimetry.

The idea behind using an ac technique has many advantages. It allows the use of signal averaging techniques to improve signal-to-noise ratio. In the determination of small changes in heat capacity, signal-to-noise ratio can become an important factor. The signal-to-noise ratio is improved because the signal which is at a particular known frequency is extracted easily from the broad-band noise. It will be shown in the next section that by a suitable choice of the reference frequency, the problem of heat loss to the surroundings can also be circumvented. This is especially advantageous for high pressure specific heat measurements, where it is impossible to reduce heat loss to the surroundings by thermal isolation, since the sample has to be in contact with the pressure transmitting medium.

## Chapter 3

### 3.2 Theory of AC Calorimetry

We give a simplified treatment of the theory of ac calorimetry. This treatment basically follows the work of Baloga and Garland [4]. The treatment given here is for the case when the heat input is given to the sample by passing a current through it. This eliminates some of the complications arising from using a separate heater. If the current that is passed through the sample is of the form

$$\mathbf{I} = I_o \sin \omega t \quad (3.3)$$

The power supplied to the sample will be

$$P = I_o^2 R \sin^2 \omega t \quad (3.4)$$

The power supplied to the sample will be partly used in increasing the temperature and part of it will be lost to the surrounding media. A heat balance equation can be written to represent such a situation.

$$m c_p \frac{dT_s}{dt} = I_o^2 R \sin^2 \omega t - k(T_s - T_b) \quad (3.5)$$

where  $T_s$  is the temperature of the sample,  $T_b$ , the temperature of the surrounding medium,  $m$  is the mass of the sample,  $C_p$  its specific heat,  $R$  is the electrical resistance and  $k$  is the thermal conductance of the surrounding medium.

This differential equation can be solved to obtain the temperature of the sample as a function of time.

$$T_s = T_b + C e^{-t/\tau} + \frac{I_o^2 R}{2k} - A \cos(2\omega t - \phi) \quad (3.6)$$

where  $A$  is given by

$$A = \frac{I_o^2 R}{2k\sqrt{1 + 4\omega^2\tau^2}} \quad (3.7)$$

and  $\phi$  is given by

$$\phi = \tan^{-1}(2\omega\tau) \quad (3.8)$$

$\tau$  is the time required for the sample temperature to relax to that of the surroundings.  $\tau$  is given by

$$\tau = \frac{m C_p}{k} \quad (3.9)$$

When  $t \rightarrow \infty$  (when steady state has been achieved), the second term in Eq. 3.6 tends to zero.  $T_s$  then consists of a constant term and an oscillatory part ( $\Delta T_{ac}$ ).

$$\Delta T_{ac} = \frac{I_o^2 R}{2k\sqrt{1 + 4\omega^2\tau^2}} \quad (3.10)$$

If the frequency  $\omega$  is chosen such that  $\omega^2\tau^2 \gg 1$ , then the equation for  $AT_{,,}$  simplifies to:

$$\Delta T_{ac} = \frac{I_o^2 R}{4m\omega C_p} \quad (3.11)$$

If the above mentioned approximation is satisfied, the heat loss to the surroundings can be effectively neglected in the calculation of the specific heat of the sample. This is one of the greatest advantages of the ac calorimetric technique.

The following points are to be noted in using this technique to calculate the specific heat:

1) The thermometer which is used should be of negligible heat capacity and should follow the instantaneous temperature of the sample.

2) The temperature gradient between the sample and the surroundings is linear. This assumption may break down at high pressures. Baloga and Garland [4] have derived the theory for ac calorimetry at high pressures starting from the one dimensional diffusion equation. Under this condition, they are not able to derive a solution for  $T_s$  in a closed form. However under certain assumptions, they are able to show that the solution reduces to a form similar to Eq. 3.11, with some additional parameters, which are determined from experiments.

3) In case an external heater is used to heat the sample, there are additional relaxation times, which have to be taken into account. This is the time taken for the sample to reach the temperature of the heater. In this case, if  $\tau_h$  is the relaxation time for the sample to reach the temperature of the surroundings, then  $\omega\tau_h \ll 1$ . To satisfy this condition the frequency has to be kept low. Since  $\omega\tau \gg 1$ , two diametrically opposite conditions have to be satisfied in this case. To make an accurate estimate of the specific heat, it may become necessary to estimate these relaxation times and include them in the calculation of the specific heat. This reduces the power of the ac calorimetric technique.

This procedure of ac calorimetry for metallic samples, was first used by Bonilla and Garland in 1974. They supplied the oscillatory heat input to the sample by passing an oscillatory current through the sample itself. In that case the time required for the sample to reach thermal equilibrium is quite small as metals have high thermal conductivity. This allows one to use quite high frequencies. Since the value of  $AT_{,,}$  is inversely proportional to frequency [4] we obtain easily measurable values of  $AT_{,,}$ . Bonilla and Garland used a heating frequency of 3.5 Hz. Bonilla and Garland found  $\tau$  to be approximately 2 sec., which gives  $\omega^2\tau^2 \simeq 66$ . In our

experiments  $\omega^2\tau^2$  was around 144, which easily satisfies the condition given above.

As can be seen from the above equations, a determination of the specific heat of the sample requires a knowledge of the resistance of the sample. Since the resistance of the sample can vary with variation in temperature or pressure, Bonnilla and Garland corrected for this variation by carrying out a separate experiment.

In our method, to be described in the subsequent chapters, we have carried out a simultaneous measurement of the sample resistance. A simultaneous measurement of the sample resistance is especially important in the case of metallic glasses, where the sample resistance can be history dependent, i.e, the sample resistance does not regain its initial value after a cycle of heating and cooling. We have also designed a constant power technique. The power dissipated in the sample is kept a constant independent of any variation in the sample resistance.

The constant power technique is important to maintain the value of  $\Delta T_{ac}$  within reasonable limits.  $\Delta T_{ac}$  is assumed to be a constant when deriving the Eqn. 3.11. In other words the value of  $C_p$  obtained is an average over the range  $\Delta T_{ac}$ . In the study of critical phenomena, it is desirable to keep  $\Delta T_{ac}$  as small as possible so as to approach very close to  $T_c$ .

### 3.3 AC Calorimetry Set-up

A schematic of the home-made experimental arrangement is shown in Fig.3.1. The entire arrangement of the ac calorimetry set-up together with the furnace for atmospheric pressure measurements and the temperature control is shown in the photograph appearing on the next page. As discussed in the previous chapter, the basic principle of ac calorimetry is to give an oscillatory heat input to the sample and measure the resulting thermal response. The instantaneous temperature of the sample has a dc part as well as an oscillatory part. The specific heat of the sample is inversely related to the amplitude of the temperature oscillations.



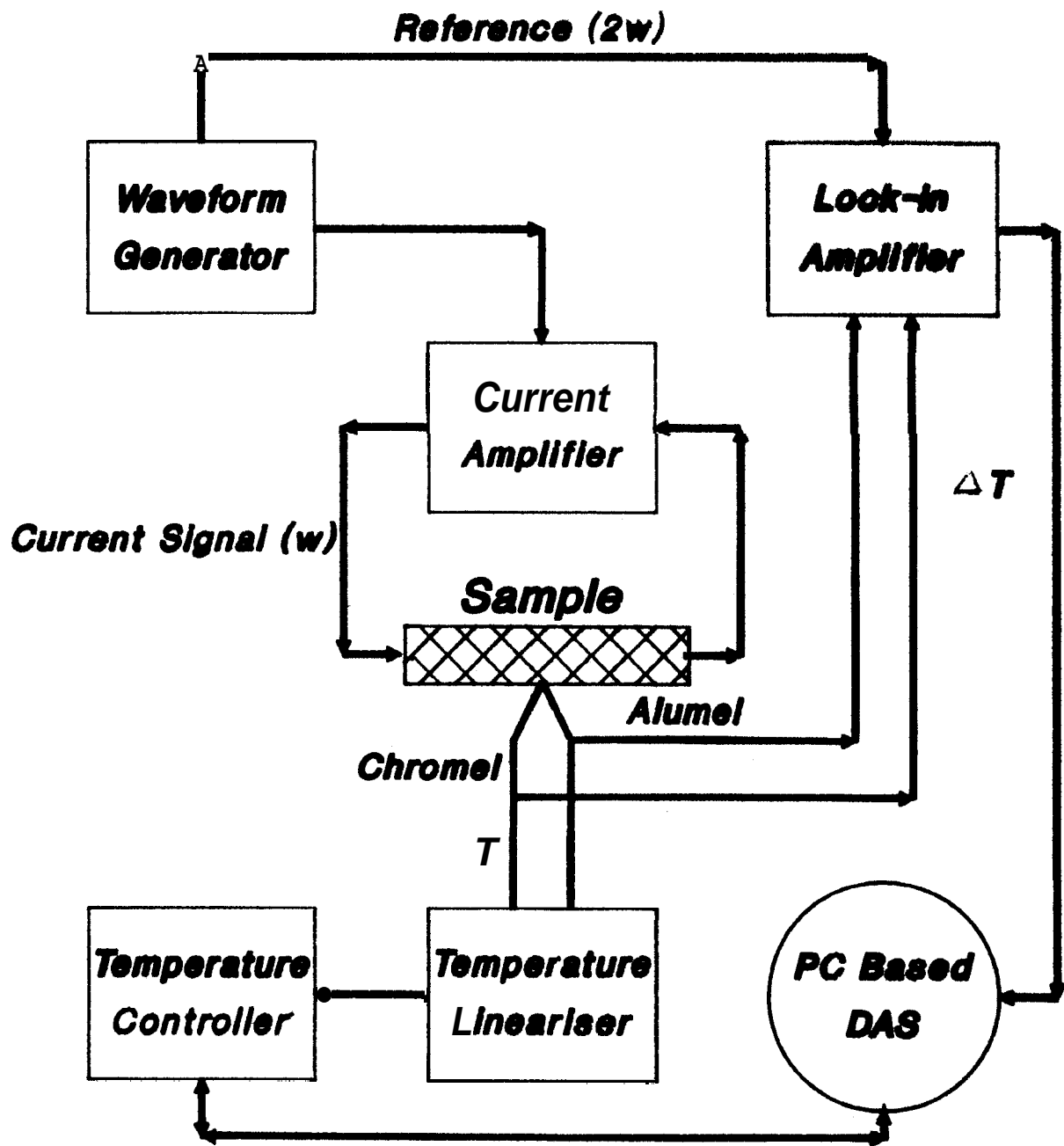


**Figure 3.1: Block Diagram of AC Calorimeter**



### Chapter 3

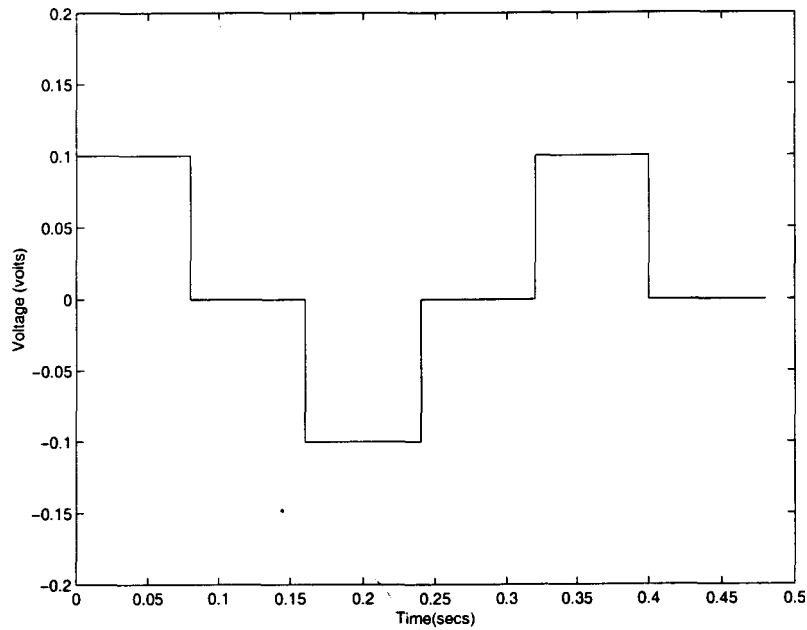


Figure 3.2: Plus-minus Square wave described in the text

---

Since the samples which are under study are all electrical conductors, the heat input is supplied to the sample by passing an oscillatory current through the sample itself. A "Plus-minus" square wave (Fig. 3.2) is used for heating the sample. A square wave is preferred over a sine wave because the second harmonic component in an ideal square wave is identically zero. The small second harmonic component which is usually present in sine wave generators can interfere with the measurement of the temperature signal which is also at the same frequency.

The absence of the second harmonic component can be proved by looking at the fourier series for this waveform.

The heating waveform can be mathematically described by the following equations:

$$\begin{aligned} I &= I_o \text{ for } t = 0 \text{ to } t = T/4 \\ I &= I_o \text{ for } t = T/4 \text{ to } t = T/2 \\ I &= -I_o \text{ for } t = T/2 \text{ to } t = 3T/4 \\ I &= 0 \text{ for } t = 3T/4 \text{ to } t = T \end{aligned}$$

### Chapter 3

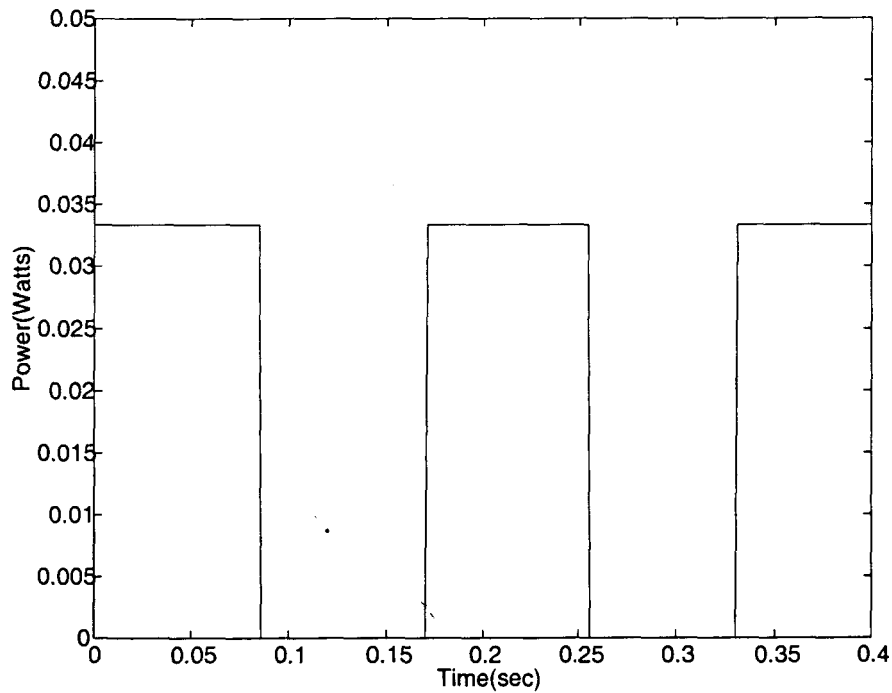


Figure 3.3: Power input to the sample vs time

This function can be split into its fourier components as follows:

$$I = \sum a_n \sin(n\omega t) + \sum b_n \cos(n\omega t) \quad (3.12)$$

$a_n$  and  $b_n$  are zero for even values of  $n$ .

The input power to the heater , which is shown in Fig. 3.3, is given by:

$$(P_o/2) + (2P_o/\pi)[\sin(2\omega t)] + (1/3) \sin(6\omega t) + (1/5) \sin(10\omega t) + \dots] \quad (3.13)$$

In contrast, the input power to a heater due to a sinusoidal heating current  $\mathbf{I} = \mathbf{I}_m \sin(\omega t)$  is

$$(P_o/2) + (P_o/2) \sin(2\omega t + 3\pi/2) \quad (3.14)$$

As a result, the plus-minus square wave current will produce, at  $2\omega$ , an ac heating effect  $(4/\pi)$  times that produced by a sinusoidal heating current of the same amplitude.

The plus-minus square wave is generated using digital techniques. The circuit of the square wave generator is given in Fig. 3.4.

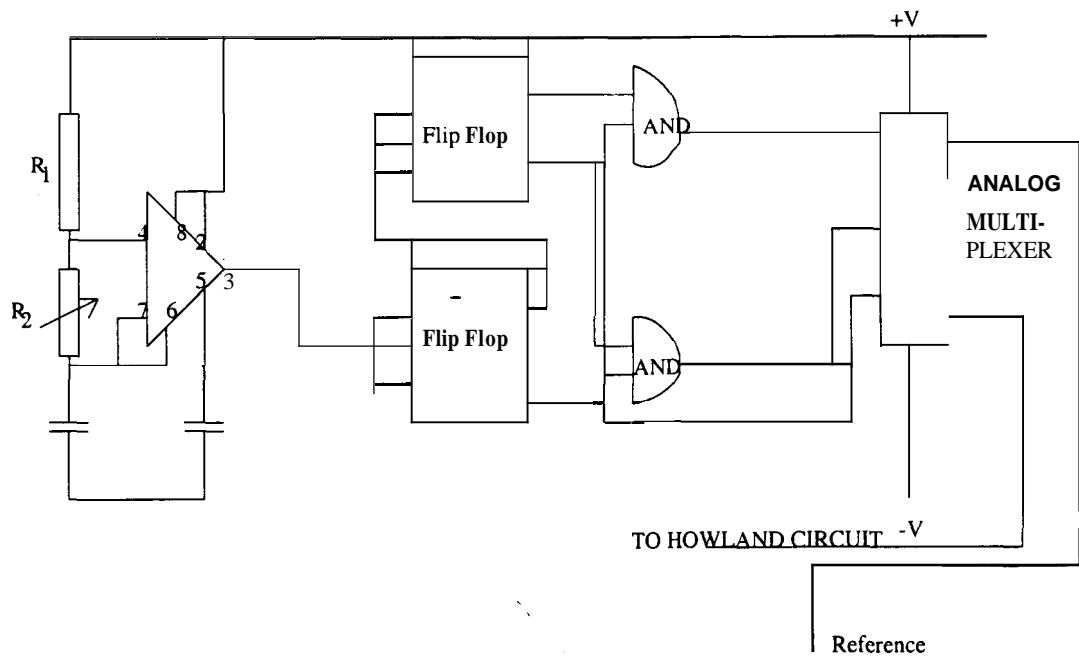


Figure 3.4: Circuit diagram of the square wave generator

### 3.4 Circuit operation

The 555 timer generates pulses as shown in Fig. 3.5. These pulses are passed through the first flip-flop. The flip-flop converts the pulses into a square wave of period  $2T$ , where  $T$  is the time period of the pulse

$$i.e., T = t_{on} + t_{off}$$

The second flip-flop doubles the period once more. The period doubling happens in the flip-flop because the output of the flip-flop changes state only when the input changes from '1' to '0' and not vice-versa.

The next stage of the circuit consists of two AND gates, which generate the outputs  $SW_1 = Q_2 \cdot \overline{Q_1}$  and  $SW_2 = \overline{Q_2} \cdot \overline{Q_1}$ . These two outputs  $SW_1$  and  $SW_2$  are the control voltages for the analog multiplexer, which operates using a  $+15, -15$  power supply.

When  $SW_1 = 1$ ,  $+V_{in}$  is transmitted to the output of the multiplexer and  $SW_2 = 1$ ,  $-V_{in}$  is transmitted. When  $SW_1 = SW_2 = 0$ , the output is zero. Of course it can be proved logically that  $SW_1$  and  $SW_2$  are never '0' in at the same time.

By this process we get the unique type of square wave which passes successively through the states  $+V_{in}, 0, -V_{in}$ .

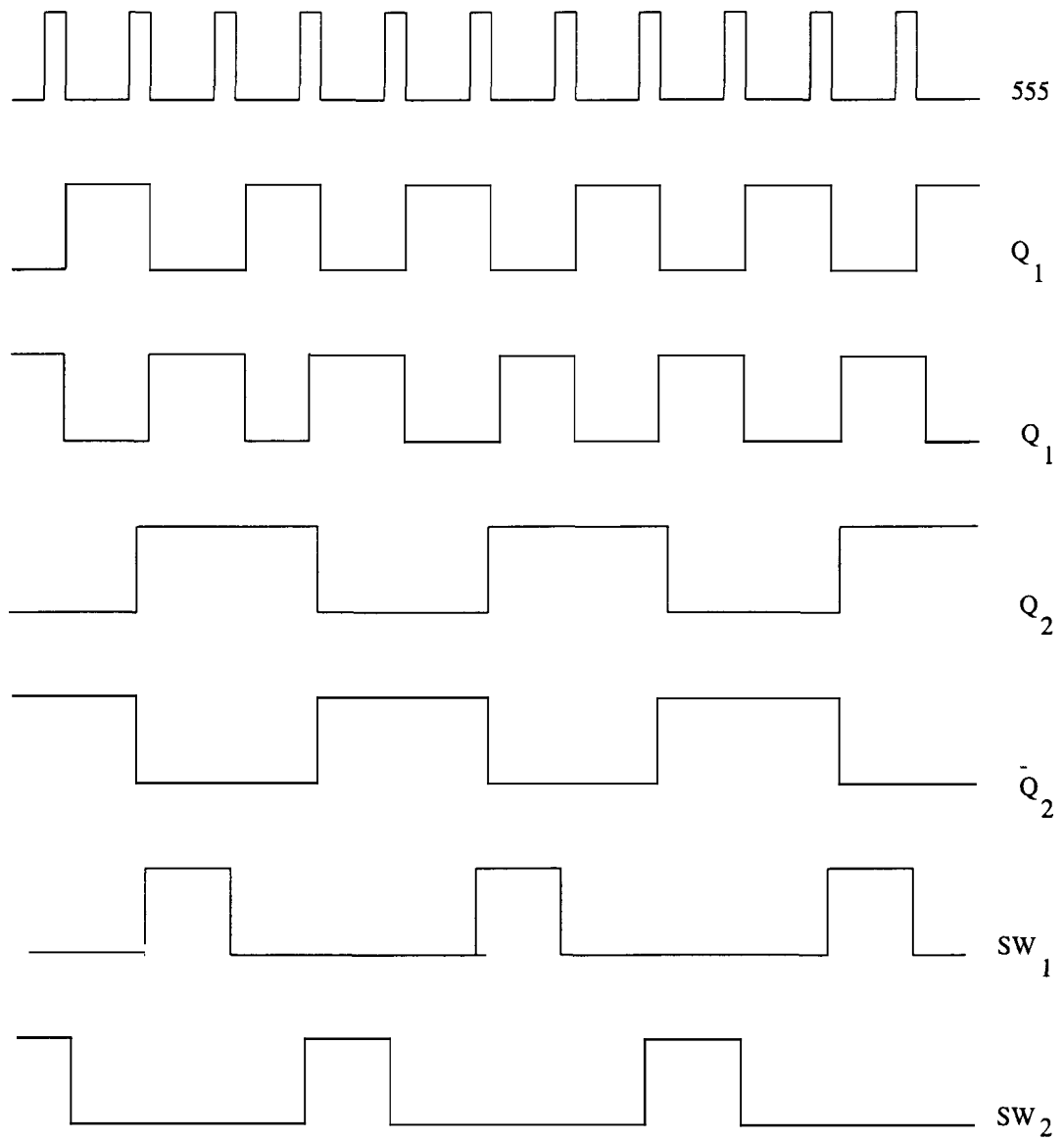


Figure 3.5: Waveforms at different stages of the square wave generator

$\overline{Q_1}$  (the negative output of the first flip-flop) is used to generate the +,- square wave as a reference for the lock-in amplifier.

All the waveforms are given in Fig. 3.5.

The output from the square wave generator is fed to the Howland circuit. The Howland circuit raises the current level in the circuit from a few mA, (which is the typical output current from the analog multiplexer) to a few amperes. A current of a few amperes is required so that the temperature oscillations in the sample are easily measurable. A high power monolithic operational amplifier (OPA 541) is used in the Howland circuit, since it has a transistor at the output stage which can provide current of the order of amperes.

### 3.5 Sample

The current from the Howland circuit is passed through the sample. The sample is either in the form of a thin wire of diameter 0.14 mm (in the case of Nickel) , or in the form of a thin foil of 20-40 $\mu m$  thickness in the case of a metallic glass. The sample should have a low thermal mass, since the amplitude of the temperature oscillations are inversely related to the mass of the sample.

The sample is held in place by a sample holder placed along the axis of a cylindrical furnace. The position of the sample is adjusted so that it is in the constant temperature zone of the furnace. A Chromel-Alumel thermocouple spot-welded at the center of the specimen is used to measure both the ac and the dc components of the temperature signal. Very thin wires are used for the thermocouple, (typically 0.01 mm diameter) as the entire heat loss from the sample is assumed to be through the surrounding medium.

The amplitude of the ac part of the temperature, the main contribution to which is at  $2\omega$ , is measured using a lock-in amplifier. Two lock-in amplifiers- 5208 PAR and SRS 830, were used in the experiments. The SRS 830 is a DSP (digital signal processing) lock-in amplifier, hence it is more immune to electrical noise and pick-up. There will also be temperature oscillations at frequencies which are odd multiples of  $2\omega$ . These will be of a much lesser magnitude than  $T_{ac}(2\omega)$ . The  $T_{ac}$  values at each temperature are recorded after allowing sufficient time for the sample to attain thermodynamic equilibrium. It is known that the equilibration time for the sample diverges near a critical point. Hence a very slow rate of heating was used near  $T_c$  (0.1°C/min). The sample temperature is maintained to within  $\pm 0.1^\circ C$  of a fixed value using a PID algorithm implemented in the software.

## Chapter 3

### 3.6 Measurement of Resistance

The calculation of the specific heat of the sample from the measured values of  $T_{ac}$  involves knowledge of the sample resistance. As mentioned earlier, Bonilla and Garland carried out a separate experiment to determine the sample resistance as a function of temperature and pressure. However in the case of metallic glasses, a simultaneous measurement of the resistance along with the specific heat is imperative since the sample resistance is history dependent, i.e, the sample resistance does not return to its initial value after a cycle of heating and cooling.

The resistance of the sample was determined by measuring the voltage across the sample using a Keithley 2001 multimeter. Two more leads are attached at the ends of the sample for the voltage measurement. Since the voltage across the sample is oscillatory, the peak value of the voltage is used for the determination of the sample resistance.

$$R = \frac{V_{peak}}{I_{peak}} \quad (3.15)$$

The peak value is determined after the voltage data has been continuously acquired for a few cycles. The voltage values whose magnitude is less than a certain threshold are rejected and the remaining values are averaged. This procedure rejects the values during the two quarters of a time-period when the waveform is zero. A finite threshold is used as the "zero" of the waveform will not be zero in practice and will have a finite spread around zero.

The values of  $\Delta T_{ac}$ , and  $R$  at each temperature are automatically recorded on a personal computer using a data-acquisition card or the IEEE 488.2 interface. The data-acquisition card has a 16 bit A/D and 16 bit D/A.

### 3.7 Constant Power arrangement

The resistance measurement outlined in the previous section can be used to obtain a constant power dissipation in the sample. Even though the resistance variation of the sample can be accounted for by substituting for  $R$  in the formula for specific heat, keeping  $I^2R$  a constant has certain advantages. The expression for  $T_{ac}$ , derived earlier, was obtained under the assumption that the specific heat of the sample is a constant over the temperature range  $\Delta T_{ac}$ . In other words the specific heat obtained using Eq. 3.18, is an average over the temperature range  $\Delta T_{ac}$ . To study critical phenomena, the sample temperature has to approach  $T_c$  as closely as possible. Hence it is advisable to keep  $\Delta T_{ac}$  as low as possible from this point of view. An optimum

value of  $\Delta T_{ac}$ , which is consistent with the above considerations and which facilitates easy detection is used.

An automatic mechanism to control the power dissipation in the sample has been used earlier by Bednarz et al [5]. However, Bednarz et al used a dedicated microprocessor based control system to achieve this, whereas our system is entirely software based and simpler to implement. The arrangement of Bednarz et al also requires knowledge of the sample resistance at the start of the experiment.

The resistance value obtained using the method detailed in the previous section is used to calculate the instantaneous power  $I^2R$ , being dissipated in the sample. The value of the current required ( $I_1$ ) to keep the power at the constant value  $P_o$ , is then computed.

An voltage equal in magnitude to  $I_1$  is then given to the input of the wave-form generator.

The entire procedure for the temperature control, measurement of  $\Delta T_{ac}$  and sample resistance is shown in the form of flowcharts in Fig. 3.6 and Fig. 3.7 respectively.

Chapter 3

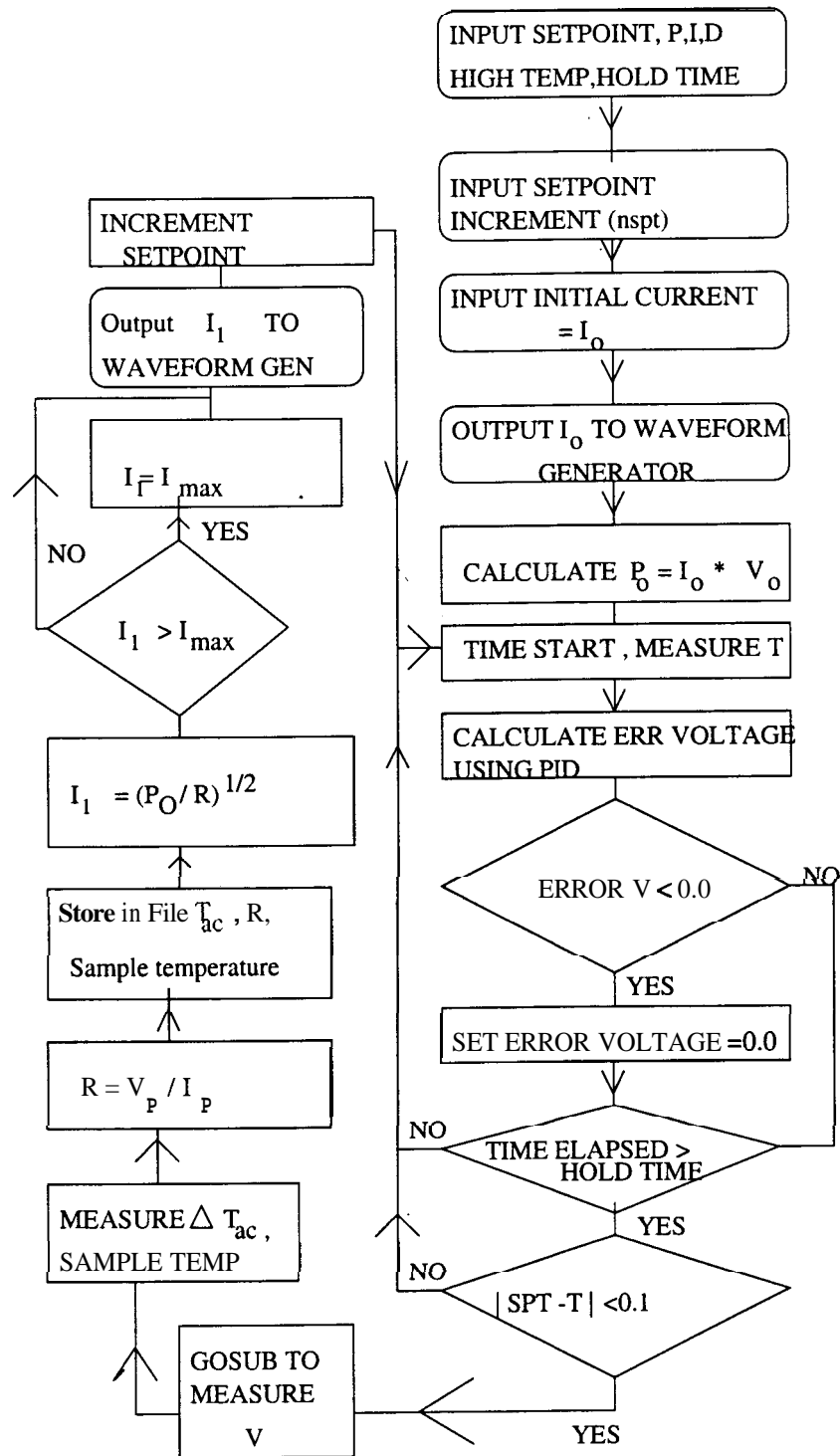


Figure 3.6: Flowchart for the operation of the ac calorimeter



## SUBROUTINE TO MEASURE V

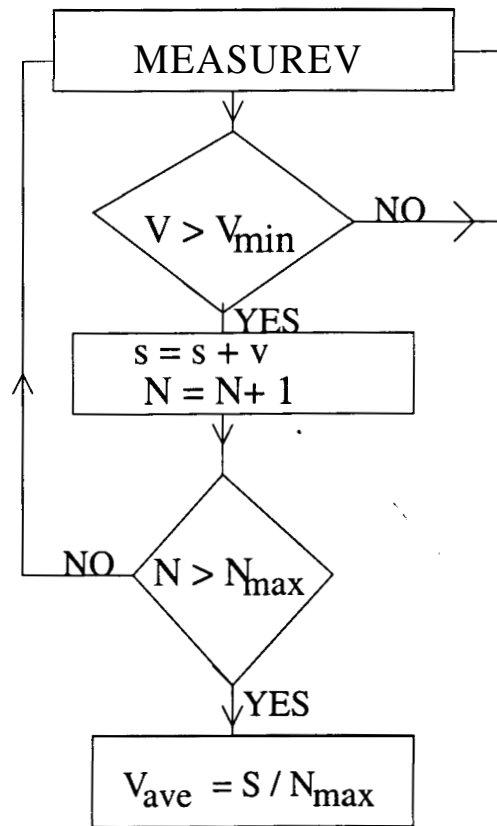


Figure 3.7: Flowchart for measurement of the sample resistance

### 3.8 Calculation of Specific Heat

According to the theory of ac calorimetry,  $T_{ac}$  is given by

$$T_{ac} = \frac{2P_o}{k\pi\sqrt{1 + 4\tau^2\omega^2}} \quad (3.16)$$

Where

$$\tau = \frac{mC_p}{k} \quad (3.17)$$

is the thermal relaxation time required for the sample temperature to relax to that of the surroundings. If the heating frequency  $\omega$  is chosen such that  $\omega^2\tau^2 \gg 1$ , then the expression for  $\Delta T_{ac}$  simplifies to

$$\Delta T_{ac} = \frac{P_o}{\pi m C_p \omega} \quad (3.18)$$

### Chapter 3

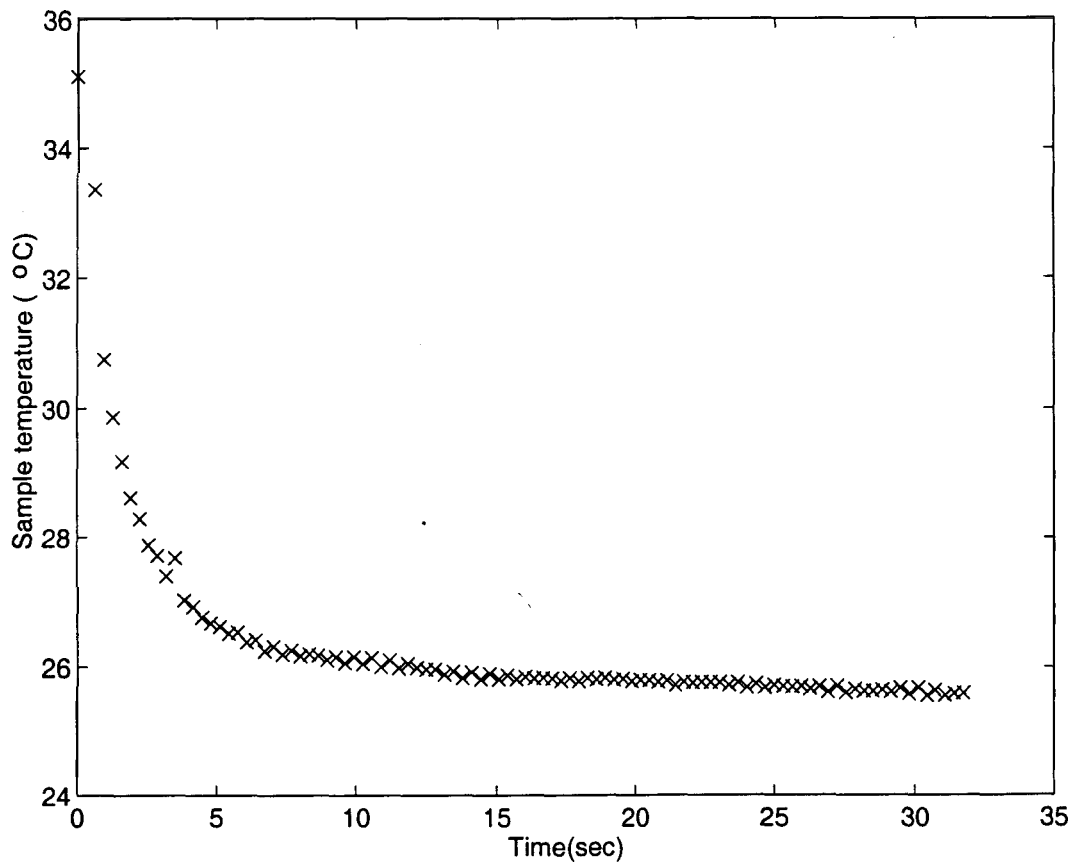


Figure 3.8: Sample temperature vs time

The value of  $\tau$  can be calculated by heating the sample to a temperature above the surrounding temperature. The heat input is then cut off and the temperature of the sample is recorded as a function of time. The temperature of the sample should decay exponentially to the surrounding temperature (Fig. 3.8) according to the equation:

$$T_s = A \exp(-t/\tau) \quad (3.19)$$

From this the value of  $\tau$  is calculated. The curve of sample temperature against time is shown in Fig. 3.8

If the sample temperature had decayed exponentially, the plot of  $\log(T-T_b)$  vs time should have been a straight line. However as seen Fig. 3.9,  $\log(T-T_b)$  vs time falls into two straight lines of different slopes. This corresponds to exponential decay with two different time constants (Eq. 3.20).

Chapter 3

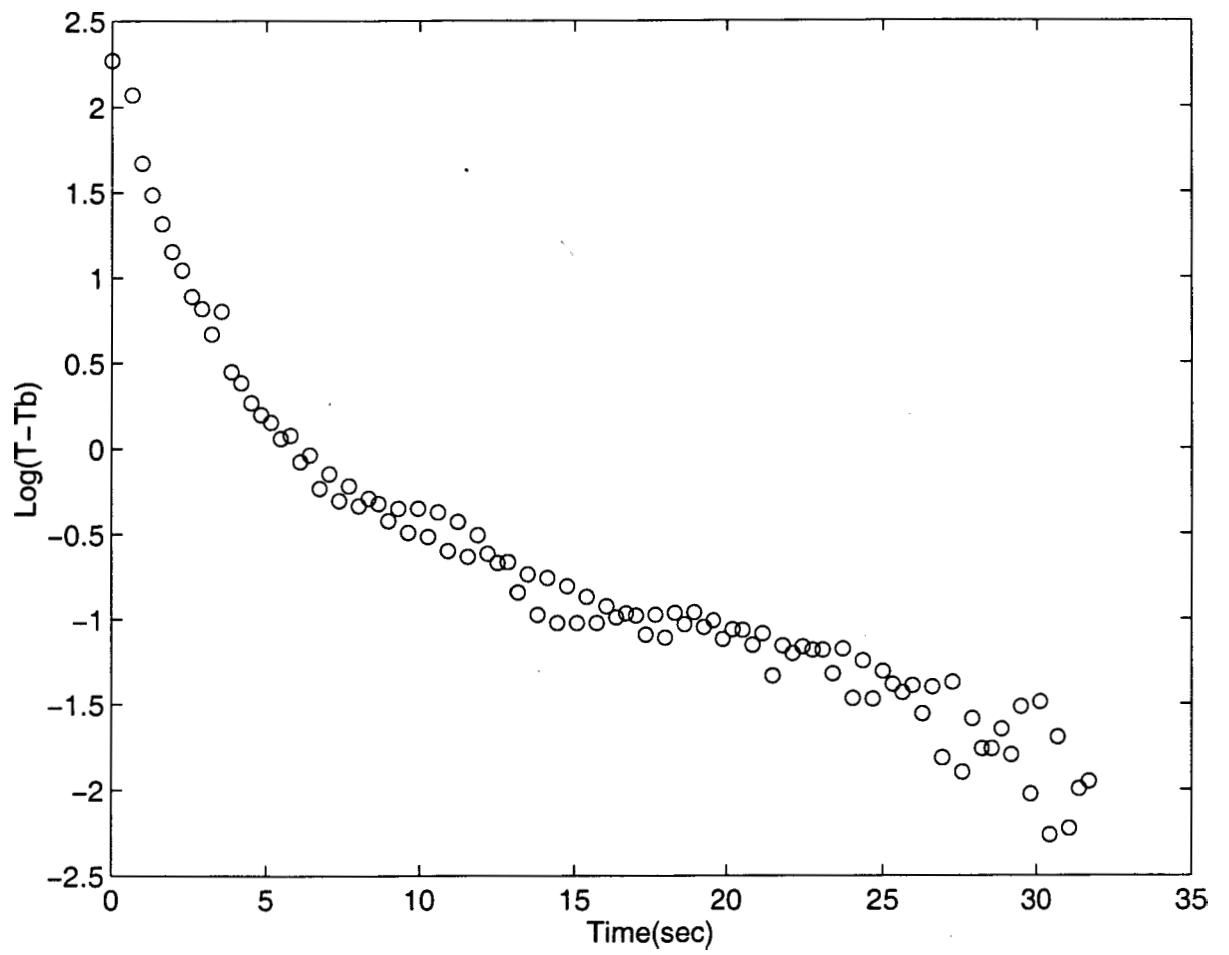


Figure 3.9: Logarithm of sample temperature vs time

### Chapter 3

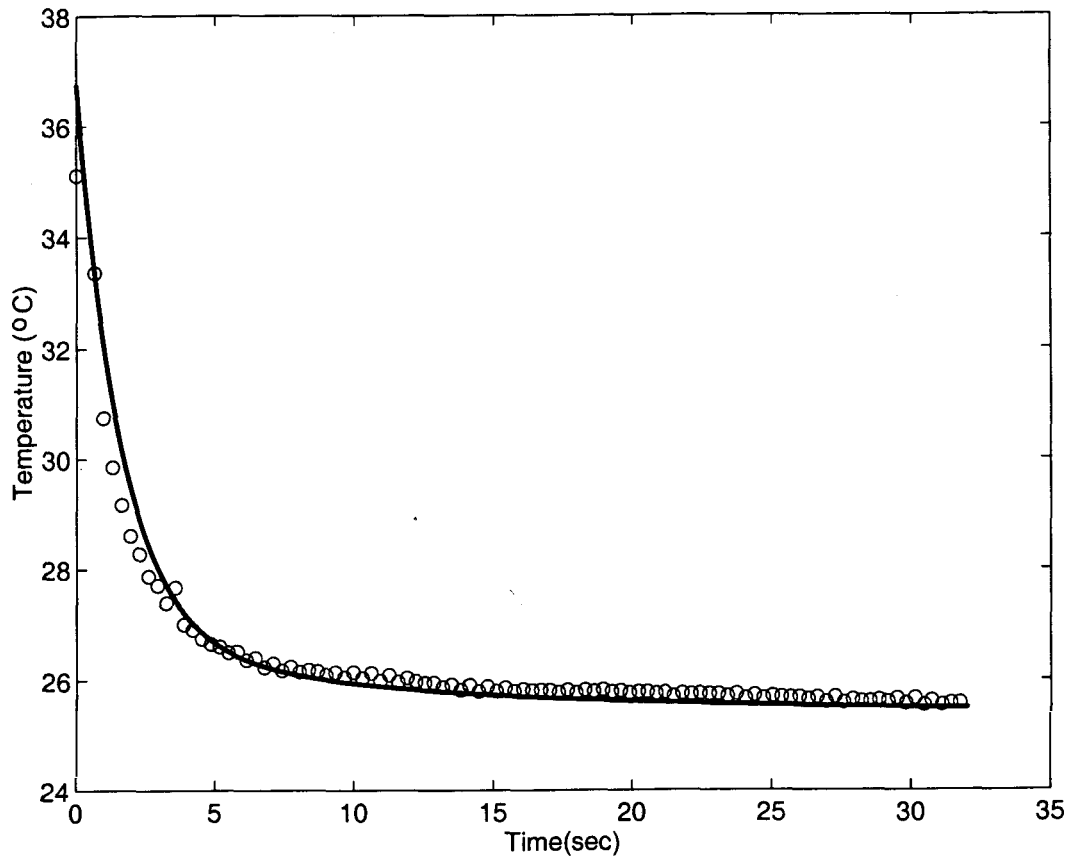


Figure 3.10: Sample temperature vs time. Solid line is a fit to Eq. 3.20

$$T_s = T_b + a_1 \exp(-t/\tau_1) + a_2 \exp(-t/\tau_2) \quad (3.20)$$

Where  $T_b$  is the temperature of the surroundings and  $\tau_1$  and  $\tau_2$  are two characteristic decay times. These two independent decay times correspond to two paths for the heat flow, i.e, one through the leads attached to the sample and one through the surrounding medium. Since the thermal conductivity of the leads is much higher than that of the surrounding medium, the time constant for heat flow through the leads,  $\tau_1$  is much lower than  $\tau_2$ .

Fig. 3.10 shows the sample temperature as a function of time. The solid line is a fit to Eq. 3.20. The parameters obtained from the fit are  $\tau_1 \sim 2$  sec and  $\tau_2 \sim 10$  sec.

Even if we use the value of  $\tau_1$  for the relaxation time, we get  $4\omega^2\tau^2 \sim \gg 1$

The condition  $\omega^2\tau^2 \gg 1$  can also be satisfied by increasing the value of  $\omega$  and  $m$ . However increasing the value of  $\omega$  and  $m$  will decrease the value of  $AT_{,,}$ .

Hence a compromise has to be struck to satisfy the condition and also to obtain a reasonable value of  $\Delta T_{ac}$ .  $\omega$  was chosen to be around 3Hz to satisfy the above conditions.

The above mentioned simplification in the expression for  $\Delta T_{ac}$  can also be obtained in a different way. The dc part of the temperature rise is given by

$$T_{dc} = \frac{P_o}{2k} \quad (3.21)$$

Substituting this in the expression for  $\Delta T_{ac}$ , we obtain an expression for the specific heat of the sample

$$C_p = \frac{P_o}{\omega m T_{ac}} \left[ 1 - \left( \frac{\Delta T_{ac}}{T_{dc}} \right)^2 \right]^{1/2} \quad (3.22)$$

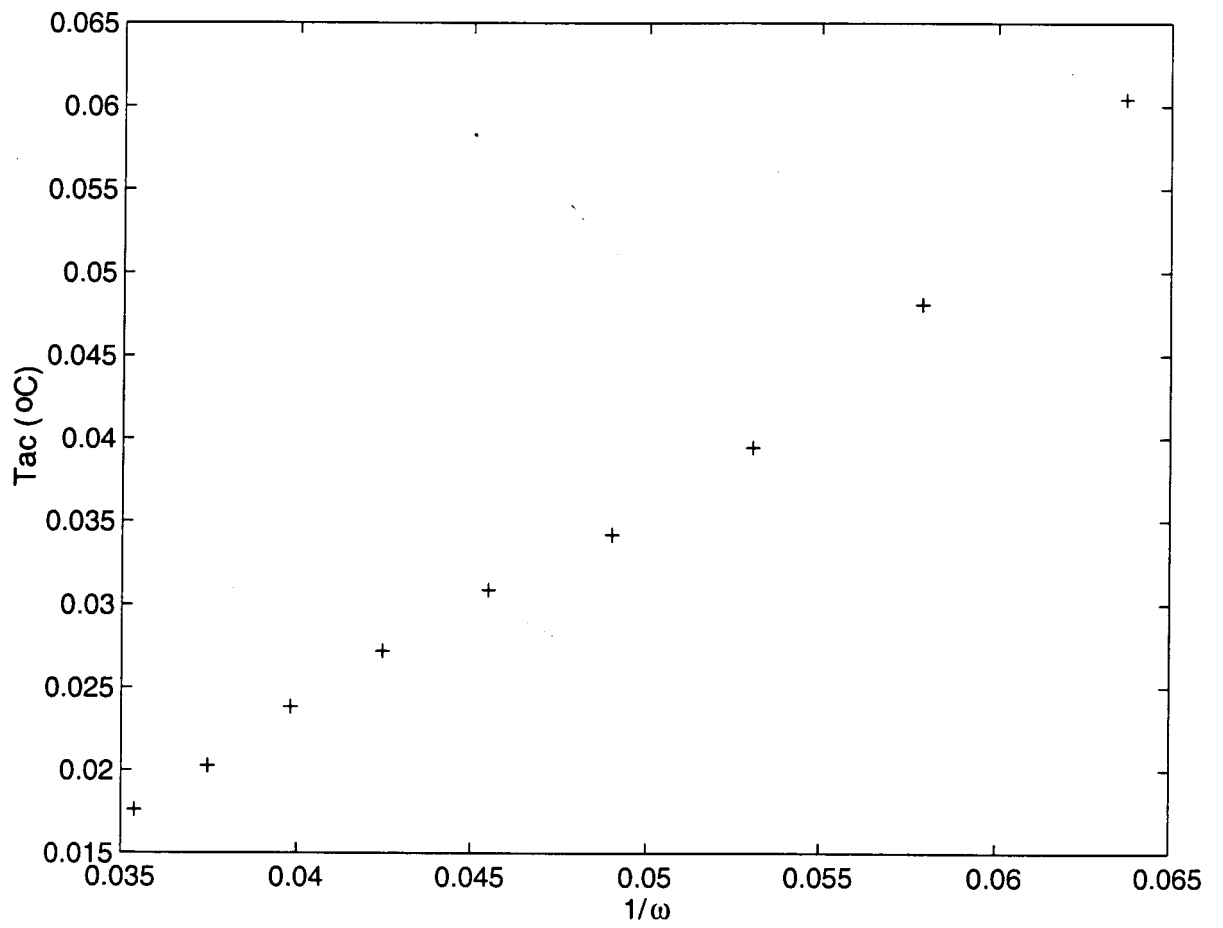
In our experiments on Nickel it was found that for  $I_o = 1$  amp  $T_{dc}$  is of the order of  $25^\circ$  and  $\Delta T_{ac}$  around  $0.1^\circ C$  at room temperature. At higher temperatures the value of  $\tau$  and hence the value of  $T_{dc}$  decreases as the thermal conductivity of the surrounding media increases with temperature. However even at  $320^\circ C$ , the value of  $T_{dc}$  is 50 times that of  $T_{ac}$  and hence the approximation involved in the calculation of  $C_p$  is still valid.

The condition  $\omega^2 \tau^2 \gg 1$  is also verified by measuring the values of  $\Delta T_{ac}$  as a function of frequency. If  $\Delta T_{ac} \sim 1/\omega$ , then the condition that  $4\omega^2 \tau^2 \gg 1$  is valid.

The values of  $\Delta T_{ac}$  was measured as a function of frequency and is shown in Fig. 3.11. It is seen from the above figure that the linear relation between  $1/\omega$  and  $\Delta T_{ac}$  is satisfied for frequencies above 3 Hz. The frequency for making the ac calorimetric measurements was chosen with this criterion in mind. If this criterion is satisfied, the heat losses to the surroundings are negligible and do not require a correction.

### 3.9 Specific Heat of Nickel

The technique described in the previous section, has been used to study the specific heat of a thin wire of Nickel ( 0.14 mm diameter and 20mm in length) in the temperature range  $30^\circ C$  to  $380^\circ C$  at atmospheric pressure. The dc part of the temperature rise is determined at the beginning of the experiment and found to be around  $25^\circ C$ .  $T_{dc}$  is around  $10^\circ C$  at  $320^\circ C$ . So the approximation involved in the determination of the specific heat is quite justified. The approximation may not work at still higher temperatures as the thermal conductivity of the surrounding

Figure 3.11:  $\Delta T_{ac}$  as a function of  $1/\omega$

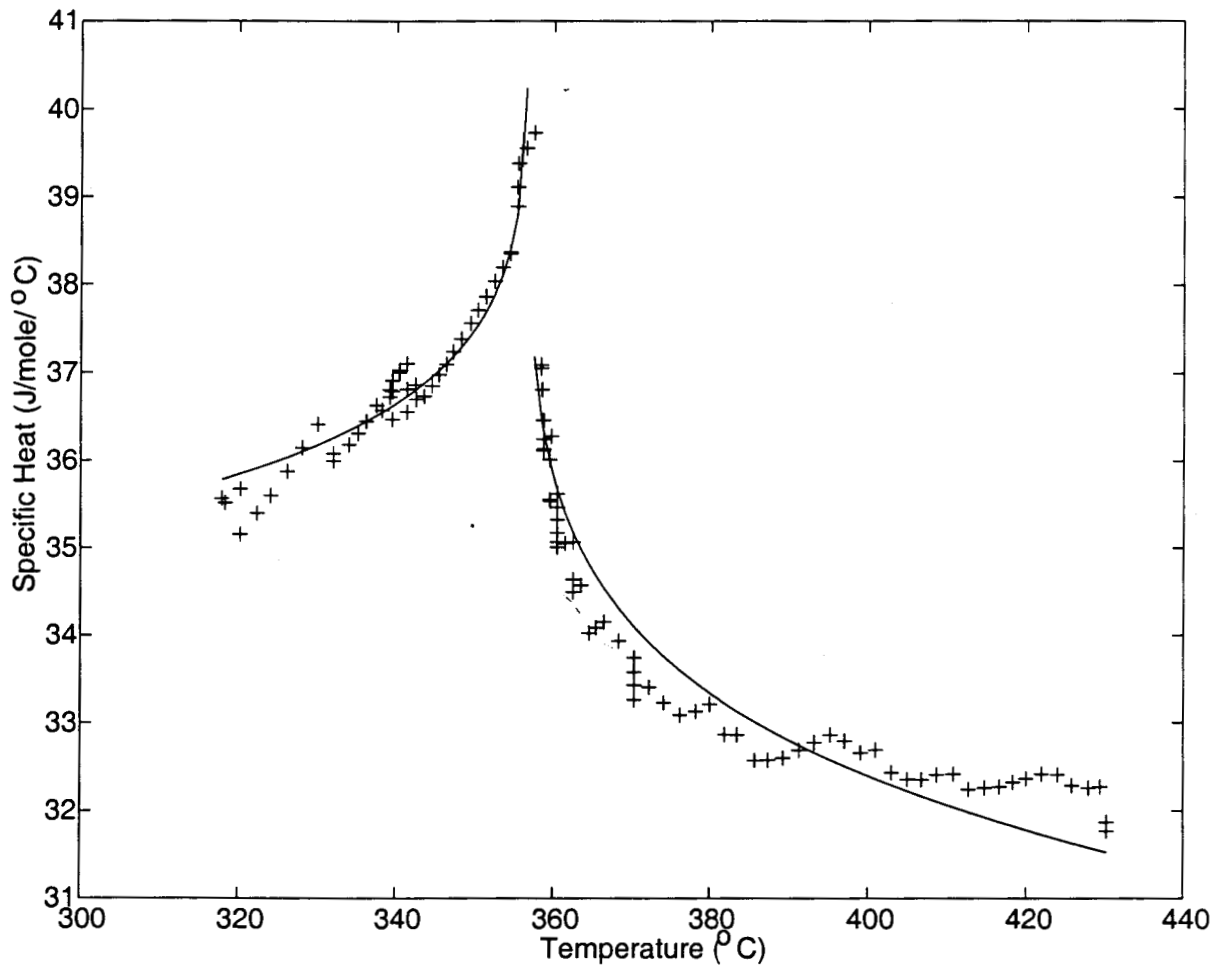


Figure 3.12: Specific Heat of Nickel near its Curie temperature. '+' - Experimental data points. Solid line is the fit of the data to Eq. 3.23

gas increases with temperature and hence the condition that  $4\omega^2\tau^2 \gg 1$  may no longer be satisfied.

In our experiment on Nickel, it was found that for  $I_o = 1$  amp and  $w = 3.15$  Hz,  $T_{dc} \sim 10^0 C$  and  $\Delta T_{ac}$  is of the order of  $0.1^0 C$ . Therefore we can neglect  $\Delta T_{ac}$  with respect to  $2T_{dc}$ .

Since we are interested only in the relative variation of specific heat, we have normalized the  $C_p$  values of Nickel with respect to the published literature values [6] to facilitate an easy comparison.

The specific heat of Nickel, measured using the ac calorimetric technique described above, is given in Fig. 3.12. The variation of  $\Delta T_{ac}$  with temperature is given in Fig. 3.13.  $T_c$  is seen as a sudden increase in the value of  $\Delta T_{ac}$ .

### Chapter 3

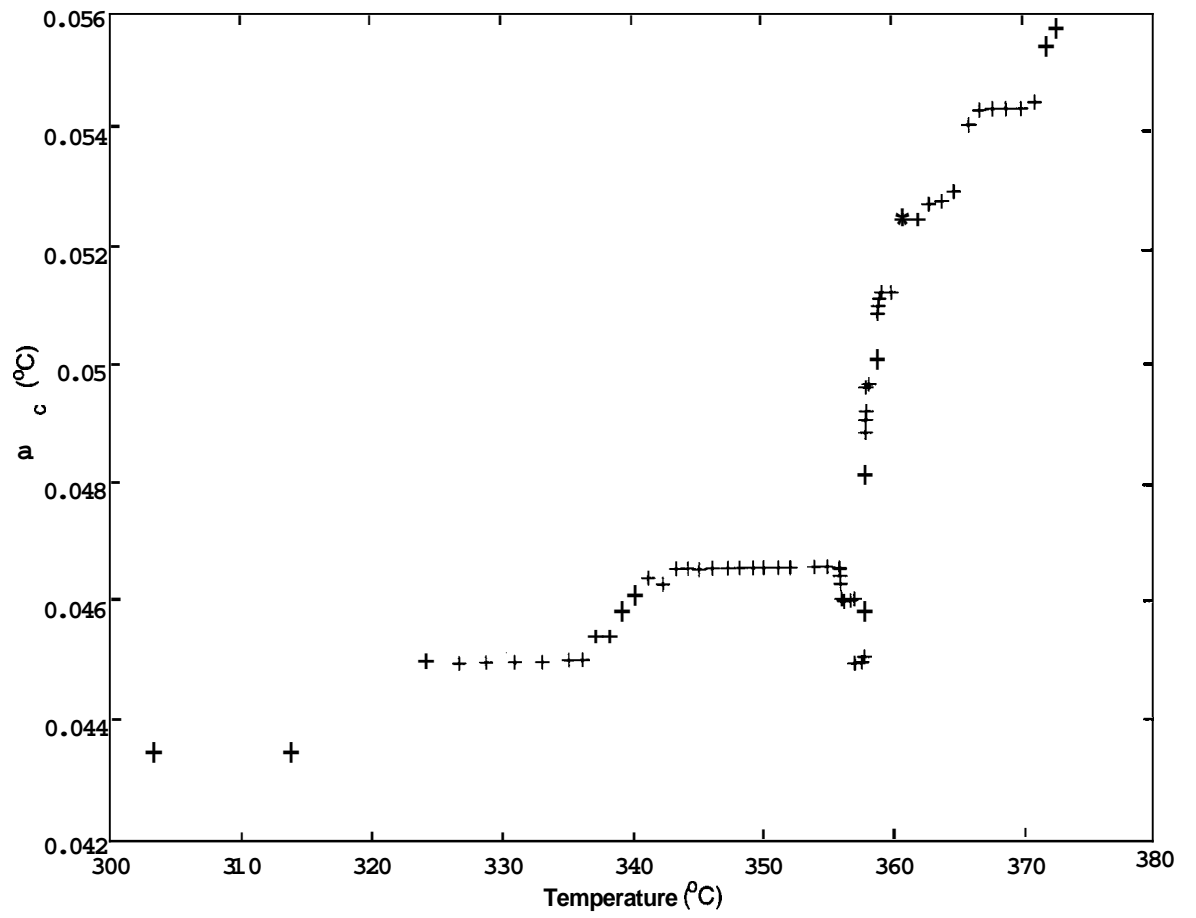


Figure 3.13: Variation of  $AT_{c,}$  with temperature for Nickel.



Chapter 3

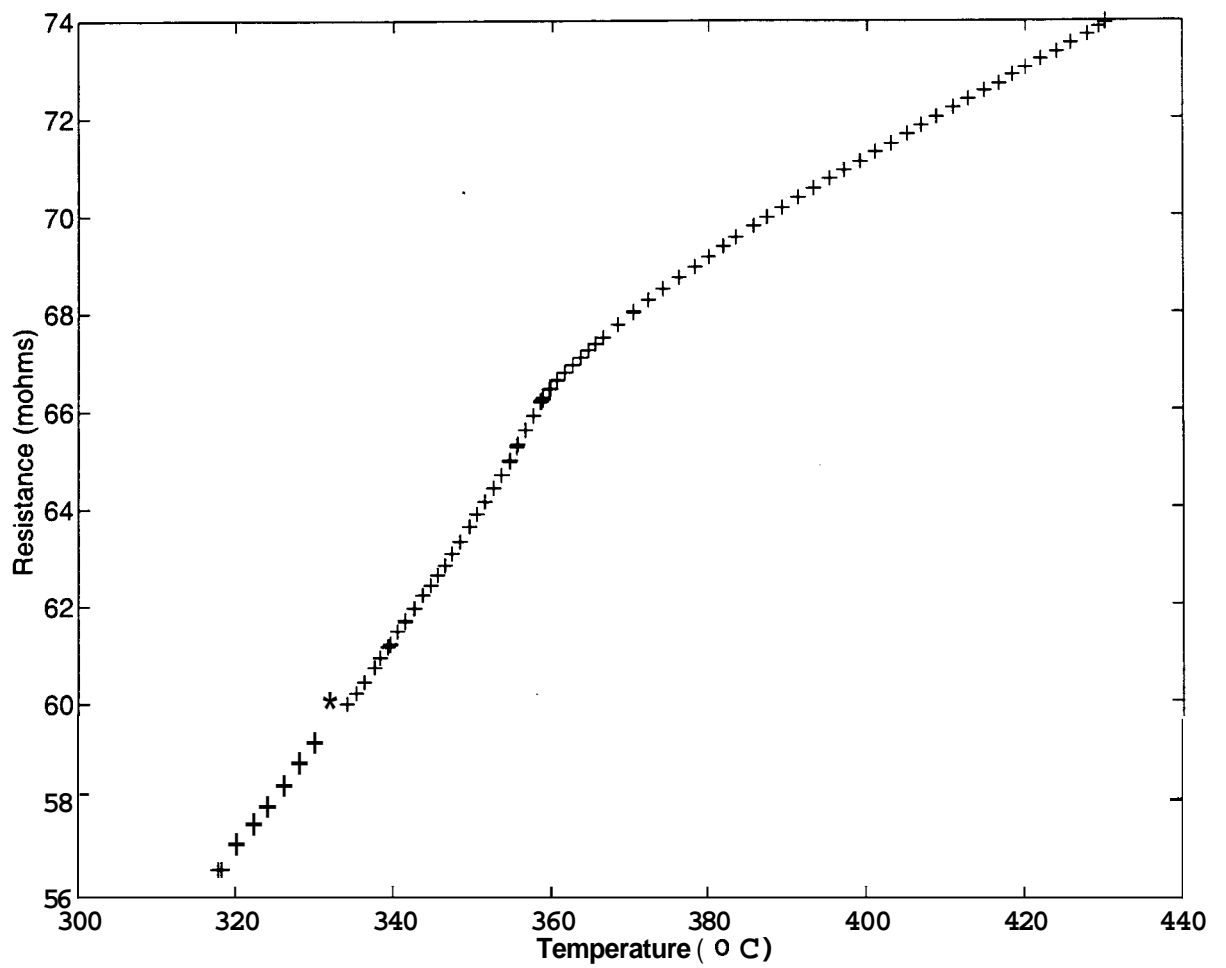


Figure 3.14: Resistance of Nickel near its Curie temperature. The Curie temperature is identified as the inflection point.

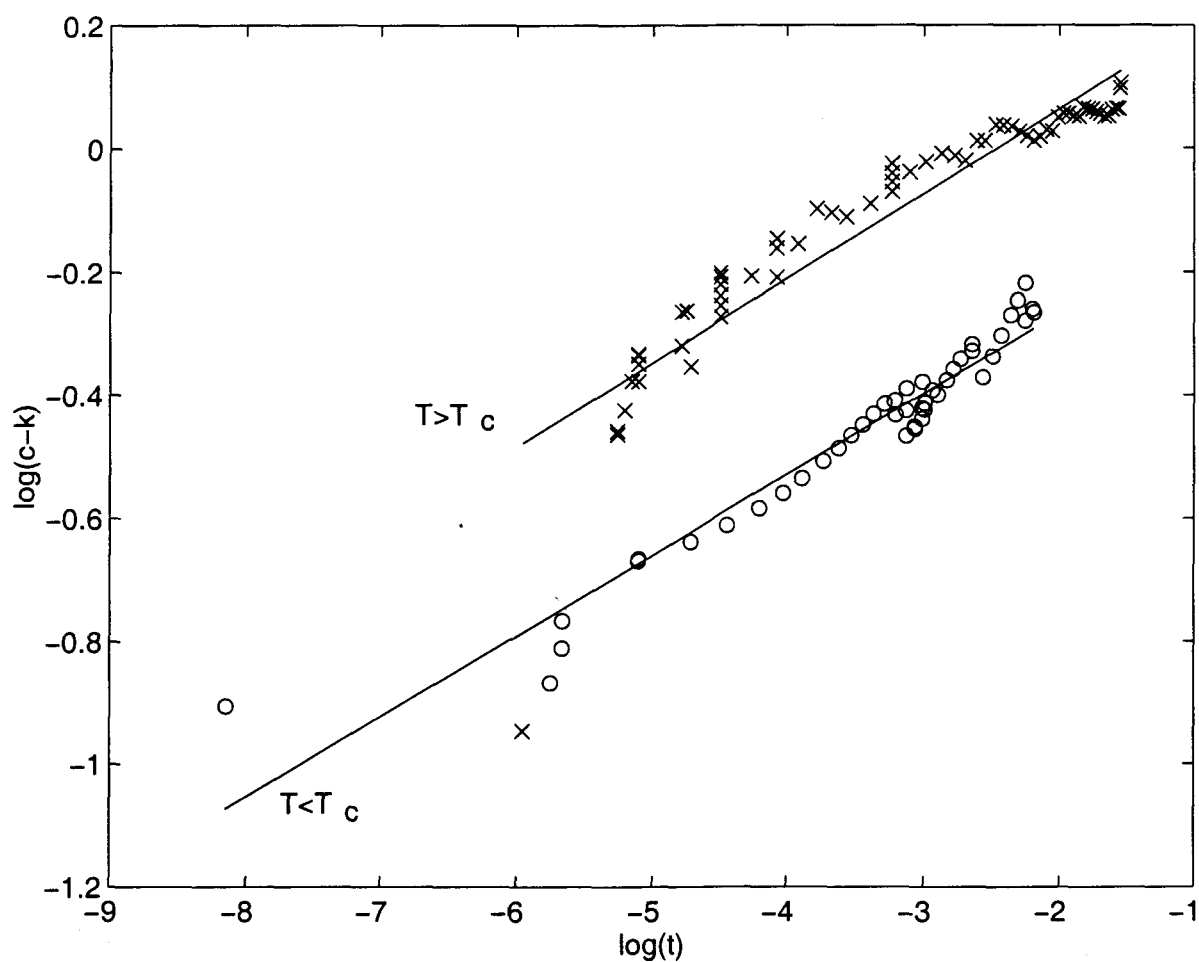


Figure 3.15: Log-Log plot of Specific heat vs temperature showing the best fit to the data for  $T < T_c$  and  $T > T_c$

The data on the resistance near the Curie temperature, obtained using the procedure described in the previous section, is given in Fig. 3.14. The correctness of our procedure is established by calculating the critical exponents that characterize the specific heat variation near  $T_c$ .

We have used an expression of the form

$$C_p = (A/\alpha)t^{-\alpha} + K \quad (3.23)$$

The exponents obtained from this fit are quite susceptible to the value of the  $T_c$  chosen. Hence in performing the fit,  $A$ ,  $\alpha$ ,  $K$  and  $T_c$  were used as adjustable parameters to get the best possible fit, shown in Fig. 3.15. The values obtained from the fit are  $\alpha = -0.13 \pm 0.03$  for  $T > T_c$  and  $T < T_c$ . These are in agreement both

with the values obtained by Connelly et al [6] as well as theoretical calculations [7]. The amplitude ratio obtained from the fit is  $A/A' \sim 1.5$  which is also in agreement with the theoretical value obtained for the Heisenberg model. The fitting was done using the MATLAB software package.

The agreement of our values with that of Connelly et al [6] also show that the specific heat of the addenda i.e, the thermocouple wires, do not contribute significantly to the measured specific heat. The relative change in the specific heat across the transition ( $\Delta C_p/C_p$ ) is approximately 12% , which is almost the same as that obtained by Connelly et al [6]. If there is a constant contribution due to the thermocouple leads this will increase the value of  $C_p$ , thereby reducing the value of  $\Delta C_p/C_p$ . Since the relative change obtained by us is of the same order as that obtained by Connelly et al [6] we infer that the contribution of the background specific heat is negligible. The quality of our data is slightly inferior to that of Connelly et al, since we they have used a slightly different method. While we have used an electrical method , they have used a pulsed light source to provide the oscillatory heat input to the sample. The optical method is less susceptible to electrical interferences and pick-ups and isolation of the measurement is easily possible. Since in our method the thermocouple is in contact with the sample through which the current is being passed it can easily pick-up stray pick-ups. Even if the lock-in amplifier can reject this noise it lengthens the measurement time. The optical method however suffers from the disadvantage that it is not convenient to get absolute values of the specific heat from the measured quantities since the fraction of the input energy which is absorbed by the sample is known. It leads to additional complications if this fraction is temperature dependent. Even though in the present work, the absolute values of the specific heat have not been calculated, the present method is more suitable for such a purpose since there are lesser number of unknown parameters.

The experimentally determined specific heat is the specific heat at constant pressure, whereas the specific heat which is calculated theoretically on the basis of the various models is the specific heat at constant volume. It has been shown by Connelly et al [6] that this does not affect the value of the exponents determined from the experimental data.

Also in the analysis of the specific heat, the lattice and electronic contributions to the specific heat were not separated from the magnetic part of the specific heat. It has been shown by Connelly et al that such a procedure does not affect the value of the critical exponents determined. The reason for this is that , while the lattice

and the electronic part of the specific heat are very weak functions of temperature, the magnetic part of the specific heat shows a singular behaviour near  $T_c$ .

The above analysis for determination of the specific heat exponents was modified to take into account the corrections to scaling (Eq. 1.12). However the inclusion of the correction term does not seem to modify the critical exponents. This indicates that the correction terms are very small in this case. The correction term is usually included to account for the presence of an *irrelevant* variable. In the case of magnetic systems, the *irrelevant* variable could be magnetic anisotropy.

The above analysis also fails to reveal a shift in the value of the exponent towards the mean field value as reported recently by Seeger et al [8].

### 3.10 Specific Heat of Nickel at High Pressures

To check the suitability of the ac calorimetric technique described in the previous section for high pressure work, the specific heat of a thin Nickel wire was measured as a function of temperature at different pressures using the piston-cylinder apparatus. The sample was placed in a high temperature cell similar to the one described in chapter 2.

Due to the difficulty in taking out 6 leads out of the high pressure cell the high pressure specific heat measurements were carried out without the simultaneous measurement of resistance. The specific heat was calculated using resistance data which was obtained through a separate experiment. The specific heat of Nickel was measured in the temperature range 30° C to 400° C. The specific heat was measured keeping the pressure constant at 1.5, 10, 15 and 20 kbars. The increase in the Curie temperature with increase in pressure can be clearly seen from the data (Fig. 3.16).

From these experiments, the value of  $dT_c/dP$  was found to be  $\approx +0.6^\circ \text{C/kbar}$ . This is slightly higher than the value ( $\approx 0.4^\circ \text{C/kbar}$ ) obtained by Leger et al [9].

According to the itinerant electron model of Lang and Ehrenreich [11],  $dT_c/dP$  is the sum of largely cancelling contributions due to the increase of the interaction and the decrease of the density of states with pressure.

The variation of  $T_c$  with pressure is discussed in detail in chapter 5. Here we give only the final expression for  $dT_c/dP$ .

$$dT_c/dP = \frac{5}{3}\kappa T_c - \alpha/T_c \quad (3.24)$$

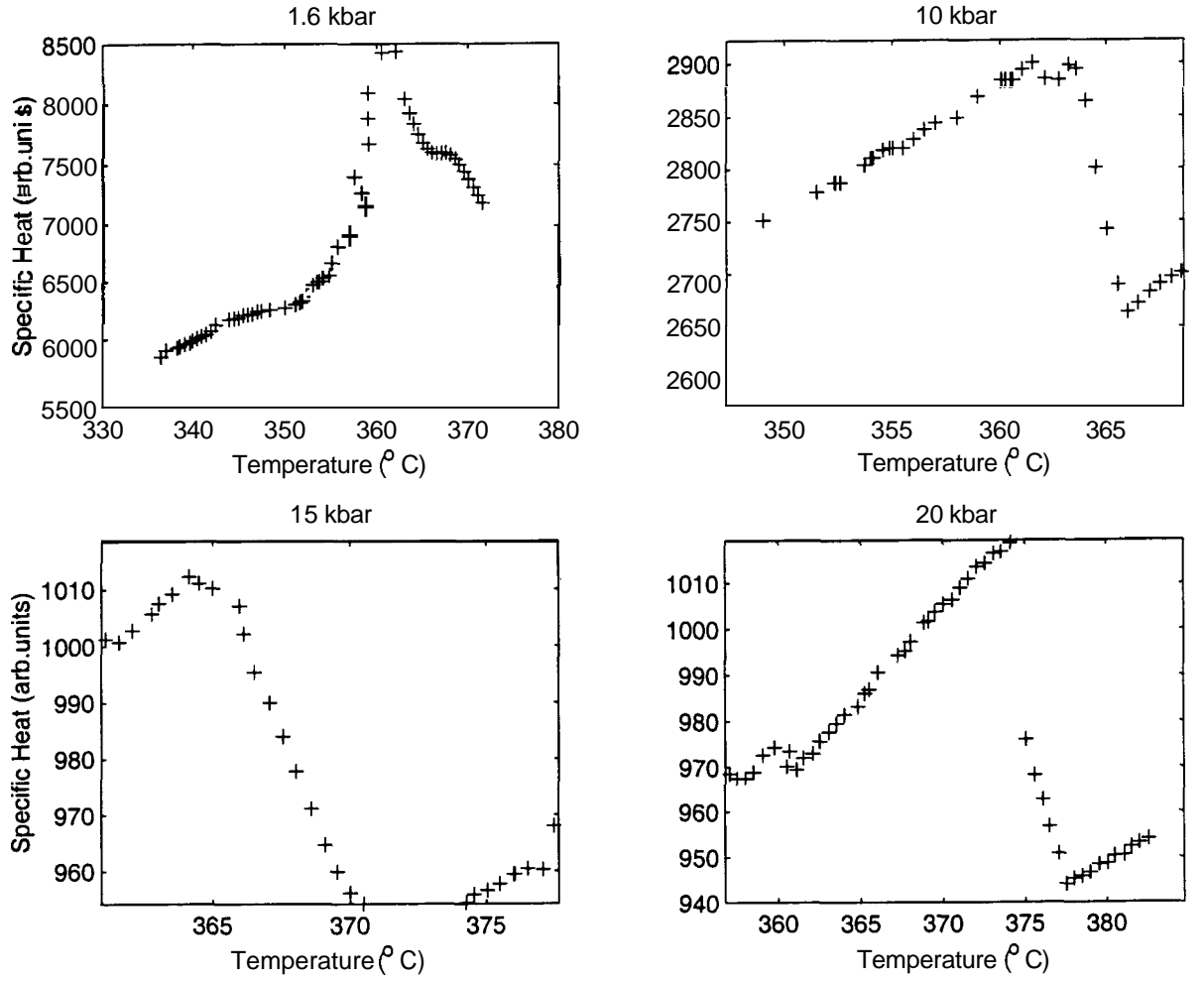


Figure 3.16: Specific Heat of Nickel as a function of temperature at different pressures

where  $\kappa$  is the compressibility and  $a$  is given by

$$\alpha = \frac{5}{6} \kappa \frac{I}{I_0} T_F^2 \quad (3.25)$$

$T_F$  is the Fermi temperature.  $\mathbf{I}$  is the interaction between electrons and  $\mathbf{I}$  is the interaction corrected for correlation effects.

In the present case since  $dT_c/dP$  is positive, the first term in Eq. 3.24 should dominate over the second term.

From Fig. 3.16, the values of  $T_c$  and the magnitude of the change in specific heat at the transition is determined and tabulated in table. 3.1.

It is seen from the above table that the magnitude of the specific heat change progressively decreases with pressure and also that the initial rate of decrease is

## Chapter 3

Table 3.1:  $T_c$  and  $\Delta C_v/C_v$  as a function of pressure

Pressure (bar)	$T_c$ °C	$\Delta C/C(\%)$
1	358	14.7
1600	359	9.52
10000	360	8.45
15000	364	6.03
20000	374	7.75

higher.

According to Landau theory, the discontinuity in the specific heat at the transition is given by

$$\Delta C_v = \frac{a_o^2 T_c}{b} \quad (3.26)$$

In the above equation,  $b$ , is usually taken to be independent of temperature. However  $b$  is in fact weakly dependent on temperature [10].

$$b = \frac{5}{24} \frac{J^4}{(kT)^3} \quad (3.27)$$

where  $J$  is the strength of interaction between the spins. Substituting Eq. 3.27 in Eq. 3.26 we have

$$\Delta C_v = \frac{3}{20} \frac{k^3 T_c^2}{J^2} \quad (3.28)$$

According to mean field theory  $J$  and  $T_c$  are connected by the relation

$$J = \frac{3kT_c}{2zS(S+1)} \quad (3.29)$$

where  $S$  is the spin on each site and  $z$  is the number of nearest neighbours. If Eq. 3.29 is substituted in Eq. 3.28, we see that  $\Delta C_v$  should be a constant. Its only dependence is on  $z$ .  $\Delta C_v$  is directly proportional to  $z^2$ . This is physically meaningful, since more the number of nearest neighbours with which each spin interacts greater will be the change in the specific heat when this interaction is absent (above  $T_c$ ). However the mean field result derived above is inconsistent with the decrease in the magnitude of  $\Delta C_v$ , which is seen from the results of the high pressure experiments on Nickel. In fact one might expect  $\Delta C_v$  to increase with pressure, since the effective number of nearest neighbours could increase at high pressures.

## *Chapter 3*

### 3.11 Conclusions

An ac calorimeter capable of measuring the specific heat of metallic samples has been designed and developed. The working of the calorimeter has been tested by measuring its frequency response and by measuring the relaxation time. The working of the calorimeter has been successfully demonstrated by measuring the specific heat of Nickel near the Curie point transition. The suitability of the ac calorimeter for High pressure studies has been demonstrated by measurements of the specific heat of Nickel at high pressures. Using these specific heat measurements, it has been possible to track the transition up to a pressure of 20 kbar. A systematic decrease in the magnitude of the specific heat change at the transition is seen with increase in pressure. It has been shown that this cannot be understood on the basis of mean field theory.

## References

- [1] C.Loriers Susse, J.P.Bastide and G.Backstrom, *Rev.Sci.Instrum.*,**44**, 1344 (1973)
- [2] M.Reading,D.Elliot and V.L.Hill, *J.Therm.Anal.*,**40**, 949 (1993)
- [3] P.F. Sullivan and G. Seidel, *Phys.Rev*, 173, 679 (1968)
- [4] Baloga and Garland, *Rev.Sci.instrum*, 48, 105 (1977)
- [5] G. Bednarz, B. Miller and M.A.White , *Rev.Sci.Instrum*, **63(8)**, 3944 (1992)
- [6] D.L.Connelly, J.S.Loonis and Mapother *Phys.Rev B*3, 924 (1971)
- [7] J.J.Binney, N.J.Dowrick, A.J.Fisher and M.E.J.Newman, *The Theory of critical phenomena*, Clarendon press, Oxford , 1992
- [8] M.Seeger, S.N.Kaul, H.Kronmuller and R.Reisser, *Phys.Rev.B*, 51, 12585 (1995)
- [9] Leger, J.M.,Susse,C., Epain,R. and Vodar,B. *Sol.Stat.Comm.* 4,197 (1966)
- [10] John Cardy, *Scaling and Renormalization in Statistical Physics*, Cambridge University Press, 1996
- [11] Lang and H.Ehrenreich,**168**, 605 (1968)